CHAPTER-IX

SUSTENANCE OF INCLUSION COMPLEXES OF IONIC LIQUID WITH CYCLIC OLIGOSACCHARIDE MOLECULES IN LIQUID AND SOLID PHASES BY DIVERSE

9.1. Introduction

Cyclodextrins (CDs) are the most common molecules used as host in case of the formation of inclusion complexes (ICs) with various guest molecules. This macromolecule especially shields the incorporated guest molecules from degradation by auto-oxidation, hydrolysis, proteolysis in solid crystalline state[1]. CDs give valuable modifications by enhancing solubility, controlling the volatility and sublimation etc.[2-5]. Due to potential applications in the field of separation, pharmaceutical and polymer science IL-CD complexes have great interest now days [2],[3].The interactions playing vital role between various ILs and α-CD, β-CD and γ-CD have been shown by means of NMR and ITC study with shown with respective binding constants[4-5]. Scientist Gao and his co-workers synthesised the solid inclusion complex of ILs of imidazolium group and CDs, which were further characterised by NMR, XRD and Mass spectroscopic methods[6]. Cyclodextrin molecules are well designed macromolecules with distinct physico-chemical properties. It has truncated cone shape with hydrophobic interior and hydrophilic exterior as the primary and secondary hydroxyl groups are present outward [7]. α-CD and β-CD contains seven glucose units with cavity diameter 4.7Å and 6.0Å respectively[8]. CD binds the guest molecule by means of hydrophobic interactions.

Published in Chemistry Select (Wiley),3(2018)7527–7534.

Ionic liquids, during the last era, have enticed the attention of the chemists due to its unique physicochemical properties and environmentally green nature and application in designing environmentally green technologies. The room temperature ionic liquids (RTILs) have been acknowledged as “novel designer materials” as its characteristics can be fine-tuned for particular purpose by changing the structure of cation and anion[9, 10]. The distinctive properties of the ILs make them suitable alternatives to classical organic solvents in various fields.

Imidazolium based ILs are of prime interest in recent but the ILs with other cationic moieties are also helpful in designing better systems. Pyridinium based ionic liquids hold interesting properties such as bactericidal and fungicidal effects, ability of interaction with peptides, oxidization inhibition efficiency and less eco-toxicity. Pyridinium based ILs are also interestingly useful in desulphurisation of fuel, extraction especially extraction of metal ion, catalysis carbon dioxide capture and dissolution of cellulose.

Here, in this work our main aim was preparation and characterisation of water soluble inclusion complex incorporating water insoluble ionic liquids 1-butyl-4-methylpyridinium hexafluorophosphate([BMPy]PF_6)α-CD and β-CD. In connection with our previous work with water soluble IL[20], we are trying to investigate the effect of anionic part in the process of inclusion complexation and prepare water soluble ICs. To investigate the formation and feasibility of ICs various physicochemical methods including the spectroscopic methods have been used.

9.2. Experimental Section

9.2.1. Source and purity of samples:

The above mentioned ionic liquid [BMPy]PF_6 and CDs were purchased from Sigma-Aldrich, Germany. The mass fraction purity of [BMPy]PF_6, α-CD and β-CD were ≥0.98.

9.2.2. Apparatus and procedure

The IL was dissolved in 20% ethanol water mixture (v/v). In this purpose triply distilled water was used and the pure ethanol purchased from Merck, India. Ethanol was used after purification. All the solutions were prepared in 20% ethanol-water mixture and used as stock. Mass of the solid IL and CDs were taken using Mettler Toledo AG-285 with uncertainty of ±0.0001gand the solutions were prepared by mass dilution at 298.15 K. Precautions were taken to reduce the evaporation during mixing.

Surface tensions of the prepared solutions were measured by platinum ring detachment technique using a Tensiometer (K9, KRUSS; Germany) at 298.15 K and accuracy was ±0.1 mN m^{-1}. Temperature was maintained by using circulating thermostated water through a double-walled glass vessel containing the solution.

Conductivities of the prepared solutions were studied using Mettler Toledo Seven Multi conductivity meter with uncertainty of ±1.0 µSm^{-1}. Measurement was performed in a thermostated water bath at 298.15 K with uncertainty ±0.01 K. The conductivity cell was calibrated by freshly prepared 0.01 M aqueous KCl solution.

^{1}H NMR spectra of the solid inclusion complex prepared were recorded in D_2O using Bruker ADVANCE 400 MHz instrument. Signals are presented as values in ppm using residual protonated solvent signal at 4.79ppm in D_2O as internal standard and all the Data are reported as chemical shift.

UV–visible spectroscopic study was carried out using JASCO V-530 UV/VIS Spectro-photometer with wavelength accuracy of ±0.5nm. Spectra were recorded at (297.15±1)K.

FT-IR spectra of the solid ICs were recorded by Perkin Elmer FT-IR Spectrometer using KBr desk procedure with scanning range 200 to 4000 cm^{-1}.

The Mass Spectroscopic analyses were done by JEOL GC MATE II quadruple double focusing mass analyser using electron impact ionization.

9.2.3. Preparation of Solid Inclusion Complex:

To prepare solid inclusion complex 1.34g of β-CD were dissolved in 30 ml of triply distilled and degassed water in round bottom flasks. The mixture was stirred to make homogeneous solutions over magnetic stirrer. On the other hand solutions of [BMPy]PF_6 was prepared taking 0.295g of [BMPy]PF_6in a separate beaker with 15ml ethanol and stirred until homogeneous mixture were formed. After both the homogeneous mixtures are prepared, the IL solution was then added into CD solution slowly with continuous stirring and after completion of the addition the IL solution the mixture was stirred for 48 h continuously. After completion of 48 hours the mixture was allowed to cool at lower temperature while a white solid was observed. The precipitate was filtered and washed for several times. Finally, the dry white powder was obtained after drying in oven at 50 °C for 24 h. The solid inclusion complex with α-CD was prepared following the same procedure. The resultant solids of inclusion complex between IL and CD were found to dissolve in pure distilled water freely. These solids were further analysed and characterised by means of FTIR, NMR and EI-Mass spectroscopic methods.

9.3. Result and discussion:

9.3.1. JOB Plot:

Job's continuous variation method was applied to determine the stoichiometry of the inclusion complexes formed [11]. By the measurement of absorbance of a set of solutions prepared of the ILs and CD in 20% EtOH & water mixture (v/v) in the mole fraction range of 0–1 (Tables S1 and S2). Calculating ΔA × R values we plotted it against R, where ΔA signifies the difference in absorbance of the IL in the pure form and complexed form and R is [IL]/([IL] + [CD]). λmax was found at 252 nm at 298.15 K. The ratio of guest and host i.e., stoichiometry is obtained from the value of R at the maxima on the Job' Plot such as R ≈ 0.33, for 1:2 IC, R≈ 0.5 for 1:1 IC, R≈ 0.66 for 2:1 IC etc. In the experiment of IL and CD the maxima in the Job' plots were obtained at R ≈ 0.5 which is the indication of 1:1 stoichiometry of IL and CD ICs (Figure1(a). & Figure1(b).]

9.3.2. ^{1}H NMR and 2D-ROESY Study to Confirm the Inclusion Phenomena:

Inclusion complex formation between IL and CD has been explained by studying^{1}H NMR spectroscopy study [12]. Investigation by this method is mainly based on the variations of chemical shifts of protons due to change of the environment inside the cyclodextrin cavity. Encapsulation of guest molecule into the CD cavity provides hydrophobic environment which is different from the bulk of the solution. Under the condition of inclusion it follows that the phenomena of inclusion is a dynamic procedure where a fast interchange of the free and the included state exists between them. Study shows the upfield shift of protons as well as downfield shift of the IL protons which is the clear indication of presence of IL molecule inside the CD cavity (Figure2. & Table. S3). From the change of the chemical shift ($\Delta\delta$) $of\ the$ H-3 andH-5 protons of CD insertion of IL molecules into the cavity of both the CD through the wider rim rather than the narrower rim can be explained as the change in chemical shift ($\Delta\delta$) of H-3 proton present near the wider rim is considerably high than that of the H-5 protons which is present near the narrower rim (Table S4)[13].Besides this, some chemical shifts are observed for H-1, H-2,H-4 that are not considerable as well as are not the part of the hydrophobic cavity of CDs.

The principle of 2D ROESY is the interaction of the protons which are present in the close proximity of 0.4 nm range to each other to produce NMR cross peaks[14].In our study, we were investigating the inclusion of the IL inside the α-CD and β-CD nano cavity. The NMR study was carried out in D_2O. It is clear that the H-3 and H-5 protons of CDs are present inside the cavity and hence if inclusion occurs, there should be presence of such close proximity of 0.4 nm of the IL protons with H-3 and H-5 protons of CD which can produce rotating-frame nuclear over hauser effect spectroscopy (ROESY) to give cross peaks [15]

In the [Figure3. and FigureS1.]there is the presence of cross peaks of H3 and H5 protons of β-CD with H-3 and H-5 protons of the aromatic ring and H-4' protons of [BMPy]PF_6 ; and with the H3 and H5 protons of α-CD and H-1', H-1"and H-4'of [BMPy]PF_6. In the dynamic process of the inclusion the cross peaks are generated due to the insertion of the butyl chain part of the IL as well as the

aromatic ring of the IL but it is not possible of entering the second IL molecule as it is sterically unfavourable (Scheme1.). Hence in some cases aromatic part and in some cases butyl chain enters inside the cavity. This incident signifies the inclusion phenomena of the said IL into the CD cavity.

9.3.3. Surface Tension:

In host-guest chemistry the study of surface tension (γ) gives strong evidence about the inclusion phenomena as well as the stoichiometry of the inclusion complexes formed[16].The structures of the selected IL contain a charged part with a butyl group. This is insoluble in pure distilled water. This acts as a surface active agent which is echoed in the lesser γ value of their solution than pure water[17]. CDs hardly show any change in the surface tension values when dissolved in the solvent for a wide range of concentration [6,18]. Hence the change of the surface tension was due to the varying concentration of the IL molecule. Here, in this experiment the γ values of IL solutions were measured with the gradually increasing concentrations of CDs at298.15 K (TablesS5). It has been found that γ values, in both the cases, was increasing with increasing concentration of CDs and (Figure4.), may be due to the insertion of the IL molecule inside the CD cavity from the bulk forming inclusion complexes. (Scheme1.)[19]. Also at a certain concentration of CD a sudden break point arrived and after that the curve becomes almost flattened (Figure4.). It is well established that the break point (Table1)at different concentrations of CD are the indications of the respective stoichiometry [31, 32].The break point near the concentration of 5mM of CD appears due to 1:1 stoichiometry. Thus from surface tension study the formation of inclusion complex can be determined.

9.3.4. Conductivity:

The study of conductivity (κ) provides valuable information about the formation and the stoichiometry of host-guest inclusion complexes[12,17a].The conductivity of the IL solutions in the mixed solvent was recorded at three different temperatures with gradual addition of CD solution(TablesS6).The tabulated results and FigureS2, reveal a decreasing trend of conductance values which may be due to the larger size and hence lower mobility of the inclusion complex

formed[12,20]. At a concentration near 5mM of CDs in both the complexes single breaks were originated which is reflected in the conductivity plot, indicates the formation of 1:1 inclusion complexes [17a, 20b].

9.3.5. Association Constants and Thermodynamic Parameters

Study of UV-Vis spectroscopy is a strong tool to calculate the association constant (K_a) for the formation of ICs[19]. In the host guest inclusion complexation when the ILs (act as chromophore) is encapsulated inside the CD cavity from the comparatively more polar bulk, there occurs a change of the molar extinction coefficient ($\Delta\varepsilon$) of the IL [40].In this study a reasonable change of the absorbance was obtained. The changes in the values of absorbance (ΔA) of IL (at λmax = 252 nm) were recorded at three different temperatures to determine the association constants (K_a) (Tables2 and Table S8–S10)[17b].Basing on the Benesi–Hildebrand method for 1:1 host–guest ICs, double-reciprocal plots of $1/\Delta A$ against $1/[CD]$ were plotted using the following equation (FigureS3.)[11b,22].

$$\frac{1}{\Delta A} = \frac{1}{\Delta\varepsilon[V]K_a} X \frac{1}{[CD]} + \frac{1}{\Delta\varepsilon[V]} \qquad \text{(IX.1)}$$

Association constants (K_a^c) were also calculated for the inclusion complexation of IL and CD by means of conductivity study with the help of a nonlinear program[19, 23]. Basing upon the fact that the insertion of the IL inside the CD cavity change the conductivity of the solutions 23-24].

The equilibrium between [BMPy]PF_6 and β-CD can be represented as:

$$IL + CD \xleftrightarrow{Ka} IC \qquad \text{(IX.2)}$$

The equilibrium constant, K_a is represented as,

$$K_a = \frac{[IC]}{[IL][CD]} \times \frac{f(IC)}{f(IL)\,f(CD)} \qquad \text{(IX.3)}$$

Where, [IC], [IL] and [CD] are the molar concentrations of the inclusion complex, ionic liquid and cyclodextrin at equilibrium accordingly. f is the activity coefficients of the respective species. The activity coefficient of CD, f(CD), can be assumed as unity [25] as the system was dilute. According to Debye-Hückel limiting law [26], f(IL)~f(IC), Equation (2) becomes

$$K_f = \frac{[IC]}{[IL][CD]} \qquad \text{(IX.4)}$$

The association constant Ka in terms of conductivity k can be shown as [37,39]

$$K_a = \frac{[IC]}{[IL][CD]} = \frac{(\Lambda_{IL} - \Lambda_{obs})}{(\Lambda_{obs} - \Lambda_{IC})[CD]} \qquad \text{(IX.5)}$$

$$\text{Where} \quad [CD] = CD_{ad} - \frac{IL_{ad}(\Lambda_{IL} - \Lambda_{obs})}{(\Lambda_{IL} - \Lambda_{IC})} \qquad \text{(IX.6)}$$

Here, Λ_{IL} denotes the molar conductivity of the IL before addition of CD, Λ_{IC} and Λ_{obs} signify the molar conductance of the inclusion complex and the mixture, CD_{ad} *and* C_{IL} the analytical concentration of CD added and IL added respectively. The association constant of IC, K_a, and Λ_{IC} were determined by using Equations (IX.4) and (IX.5).

From the binding constant values the change in the enthalpy (ΔH^0) and entropy (ΔS^0) were calculated by plotting logK_f against 1/T according to Van't Hoff equation (IX.6) for both the CDs after calculating the association constant [Figure5(a). And Figure5(b)]. The values of ΔH^0 and ΔS^0 obtained from both the procedures are expressed in table 5. From the change of enthalpy and entropy values, the change in the Gibb's free energy has been calculated at 298.15 K using the entropy and enthalpy values.

$$2.303 \log K_f = -\frac{\Delta H^0}{RT} + \frac{\Delta S^0}{R} \qquad \text{(IX.7)}$$

The association constant obtained from the two processes signifies the feasibility of the inclusion (Table2 and Table3). The association constants at three different temperatures were used to calculate the thermodynamic properties.

The changes in enthalpy (ΔH) and entropy (ΔS)for the process of inclusion were found negative, signifies inclusion process to be exothermic and is not entropy-driven rather entropy-restricted. (Table 2 and 3)[17a]. This may be due to the molecular association during the formation of the inclusion complexes of CDs and IL. Because of this, the entropy decreases, this is contrary for the spontaneity of the formation of ICs. But this effect of entropy was overcome by the greater negative value of enthalpy change, which makes the whole process of inclusion thermodynamically favourable.

Again the spontaneity of formation of ICs can be related with free energy change (ΔG) during the process. This can be easily calculated from the thermodynamic parameter ΔH and ΔS using the following equation (IX.7) at 298.15K. The ΔG values are negative for both the ICs which indicate the feasible formation of the ICs and the complexation is an exergonic process.

$$\Delta G = \Delta H - T\Delta S \qquad \text{(IX.8)}$$

The ΔG values for the two binding partners ([BMPy]PF_6,with α-CD and β-CD) are negative ($-\Delta G$) which indicates that the host-guest IC proceeded spontaneously(Table 2 and 3) at 298.15 K and the complexation is an exergonic process.

9.3.6. Powder X-Ray Diffraction (P-XRD)

Powder XRD is another reliable tool for characterization of ICs in the solid state as it helps to detect complexation in the powder form or in microcrystalline states. The PXRD diffraction pattern of the IC becomes distinct from the diffraction pattern of pure host and guest molecules.[27] The characteristic peaks in the spectra (Figure 6.) of pure [BMPy]PF6 are obtained at 2θ (degree) 11.9411, 18.8402, 20.4822, 22.7573 and 22.8762revealed high-intensity reflection indicating its crystalline structure.[28] It is evident from the Figure 6

that the diffraction pattern of the inclusion complexes is different from the pure IL,α-CD and β-CD. The lower intensity of the complexes indicates the less crystalline nature compared to the IL. The phenomenon confirms the formation of ICs.[29]

9.3.6. FTIR:

FT-IR study of the solid ICs formed was performed to investigate the formation of the solid ICs. There are changes in frequencies of bands of the inserted guest molecules as well as some bands are absent in the spectra of complex. This may be due to the formation of the ICs[30]. Data for pure compounds and inclusion complexes are recorded in TableS11 and spectroscopic change in wave number before and after inclusion are shown in Figure7. Due to non-covalent interactions the changes of bands are observed. In the spectra of α-CD and β-CD the broad bands obtained at 3410 $cm^{-1}$and 3408 $cm^{-1}$are due to the valence vibrations of O-H groups linked by H-bond. The O-H stretching for α-CD and β-CD obtained at 3410 cm^{-1} and 3408 cm^{-1} were obtained in the complexes 3383 cm^{-1} and 3394 cm^{-1}respectively, may be due to the interaction of the positively charged nitrogen atom of the pyridine ring and the oxygen atom of O-H group which is again reflected in the shifted band of C=N stretching form 1647cm^{-1} for the pure IL to 1636cm^{-1} and 1638 cm^{-1} in the ICs of β-CD and α-CD respectively. The C-H stretching and bending are obtained at 2941cm^{-1} and 1404 $cm^{-1}$for pure β-CD and2935cm^{-1} and 1406 cm^{-1} for pure α-CD, which are shifted in the ICs to 2931 cm^{-1},1388 cm^{-1} for β-CD and 2927 cm^{-1}, 1371 $cm^{-1}$for α-CD. The out of plane C-H bending for [BMPy]PF_6 obtained at 841 cm^{-1} obtained at 830 $cm^{-1}$and 832 cm^{-1} for α-CD and β-CD respectively. This may be due to the closeness of C-H of CD and the aromatic C-H of the IL. The aromatic stretching bands for pure [BMPy]PF_6 observed at 3142cm^{-1}, stretching band due to alkyl C-H at 3068cm^{-1}, are absent in the spectra of the ICs[31]. The peak due to stretching of C-H from -CH_2- at 2965$cm^{-1}$from [BMPy]$PF_6$are absent or shifted to 2931$cm^{-1}$and 2927cm^{-1}in the spectra of ICs of β-CD and α-CD respectively, may be due to the interaction inside the cavity of cyclodextrin. In the ICs no additional signal is

obtained which denies the chance of chemical reaction[32]. Thus the study provides significant information about the formation of the ICs in the solid state.

9.3.7. Electrospray Ionization (ESI) Mass Spectrometric Analysis of Inclusion Complexes.

The inclusion complexation of the ILs with β-CD was further confirmed by studying ESI-mass spectrometry. The spectra and peaks with possible ions are shown in the (Figure S4) and Table S9.The peaks found at m/z 1268.92 and 1290.94 represent $([BMPy]PF_6$+α-CD + $H)^+$ and $([BMPy]PF_6$+ α-CD + $Na)^+$respectively, peaks found atm/z 1431.11 and 1452.87 represent$([BMPy]PF_6$+β-CD + $H)^+$ and $([BMPy]PF_6$+ β-CD + $Na)^+$, respectively. The above study confirms the formation of expected ICs, namely, $[BMPy]PF_6$+α-CD and $[BMPy]PF_6$+ β-CD, in the solid state and the stoichiometry of the host and guest is 1:1.

9.4. Conclusion:

The thorough experiment describes the formation of the inclusion phenomena of $[BMPy]PF_6$with α-Cyclodextrin and β-Cyclodextrin. The solid ICs formed were found freely soluble in pure distilled water. The Inclusion phenomena in the solid state were confirmed by 1H-NMR, FT-IR spectroscopy and Mass spectrometry. Again the inclusion phenomena and stoichiometry of the inclusion complexes formed were established by Job's plot from UV-Vis study, Surface tension and conductance study. Binding constant of the ICs calculated from UV-Vis and conductometric study, confirmed the significant association between the ILs and β-CD and good feasibility of formation of the ICs.

4.5. REFERENCES

References of CHAPTER IX are given in BIBLIOGRAPHY (Page No.303 to 306)

Tables

Table1. Values of surface tension (γ) and at the break point with corresponding concentration of α –CD, β-CD for [BMPy]PF6 at 298.15 K[a]

	Surface tension	
	[BMPy]PF_6+α-CD	[BMPy]PF_6+β-CD
Conc. Of CD/ mM	5.020538567	5.106856634
γ/mN m^{-1}	41.98741944	41.8830187

[a]Standard uncertainties in temperature u are: u(T) = 0.01 K.

[a]Standard uncertainties in temperature: ± 0.01 K, Pressure: ± 10kPa, surface tension: ±0.02mNm^{-1}

Table2. Association constants obtained by the Benesi–Hildebrand method (K_a)from UV-Vis study and corresponding thermodynamic parameters and stoichiometry of [BMPy]PF_6 & α-CD and [BMPy]PF_6& β-CD inclusion complexes at 293.15K[a], 303.15K[a] at 313.15K[a].

	$k_a(10^{-3}M^{-1})$			ΔG^0 (kJ mol^{-1})	ΔH^0 (kJ mol^{-1})	ΔS^0 (J mol^{-1}) K^{-1}
	293.15K	303.15K	313.15K			
[BMPy]PF_6 & α-CD	6.24	4.32	2.82	-21.20	-30.29	-30.51
[BMPy]PF_6 & β-CD	4.64	3.22	2.23	-20.46	-27.95	-25.12

[a]Standard uncertainties in temperature: ± 0.01 K, Pressure: ± 10kPa.

Table3. Association constants obtained by the nonlinear program (K_a^c) from conductance study and corresponding thermodynamic parameters and stoichiometry of [BMPy]PF_6 & α-CD and [BMPy]PF_6& β-CD inclusion complexes at 293.15K[a], 303.15K[a] at 313.15K[a].

	$K_a^c(10^{-3}M^{-1})$			ΔG^0	ΔH^0	ΔS^0
	293.15K	303.15K	313.15K	(kJ mol^{-1})	(kJ mol^{-1})	(J mol^{-1}) K^{-1}
[BMPy]PF_6 & α-CD	6.16	4.26	2.79	-21.16	-30.20	-30.34
[BMPy]PF_6 & β-CD	4.57	3.16	2.20	-20.43	-27.85	-24.91

[a]Standard uncertainties in temperature: ± 0.01 K, Pressure: ± 10kPa.

TableS1. Data for Job's Plot performed by UV-Vis spectroscopy for [BMPy]PF_6-β-CD system at 298.15 K [a]

IL conc. [IL] (µm)	β-CD (µm)	R= [IL]/ ([IL]+[β-CD])	A @λmax 252 nm	ΔA (0.48172-A)	ΔAx[D]/ ([D]+[β-CD])
0	100	0	0.0714	0.47472	0
10	90	0.1	0.1108	0.36384	0.036384
20	80	0.2	0.1547	0.31999	0.063998
30	70	0.3	0.1968	0.27784	0.083352
40	60	0.4	0.2346	0.2401	0.09604
50	50	0.5	0.2738	0.20086	0.10043
60	40	0.6	0.3195	0.1552	0.09312
70	30	0.7	0.3615	0.11318	0.079226
80	20	0.8	0.4050	0.06963	0.055704
90	10	0.9	0.4505	0.02422	0.021798
100	0	1	0.4747	0	0

[a]Standard uncertainties in temperature u are: (T) =±0.01K

TableS2. Data for Job's Plot performed by UV-Vis spectroscopy for [BMPy]PF_6-α-CD system at 298.15 K [a]

drug conc. [D] (µm)	α-CD (µm)	R= [D]/ ([D]+[αcd])	A @λmax 252 nm	ΔA (0.48172-A)	ΔAx[D]/ ([D]+[α - CD])
0	100	0.0	0	0.47472	0
10	90	0.1	0.11415	0.36057	0.036057
20	80	0.2	0.1467	0.32802	0.065604
30	70	0.3	0.18321	0.29151	0.087453
40	60	0.4	0.23243	0.24229	0.096916
50	50	0.5	0.26294	0.21178	0.10589
60	40	0.6	0.31581	0.15891	0.095346
70	30	0.7	0.36474	0.10998	0.076986
80	20	0.8	0.39745	0.07727	0.061816
90	10	0.9	0.44861	0.02611	0.023499
100	0	1.0	0.47472	0	0

aStandard uncertainties in temperature u are: (T) =±0.01K

TableS3. 1H-NMR spectra of [BMPy]PF_6, α-CD, β-CD, and [BMPy]PF_6+α-CD, [BMPy]PF_6+β-CD complexes.

α-Cyclodextrin (400 MHz, Solvated in D_2O) δ /ppm	β-Cyclodextrin (400 MHz, Solvated in D_2O) δ /ppm
3.41-3.44 (6H, t, J= 9.00 Hz), 3.45-3.51 (6H, dd, J= 10.00, 3.00 Hz), 3.73-3.89 (18H, m), 3.81-3.87(6H,t, J = 9 Hz), 4.89-4.94 (6H, d, J = 3 Hz)	3.41-3.47 (6H, t, J = 9.2 Hz), 3.48-3.53 (6H, dd, J =9.6, 3.2 Hz), 3.72-3.77 (18H, m), 3.79-3.86 (6H,t,J=9.2 Hz), 4.91-4.95 (6H, d, J = 3.6 Hz).
[BMPy]PF_6	
0.77-0.81(3H, t, J=8Hz); 1.15-1.25(2H, m); 1.78-1.86(2H, dd, J=8Hz); 2.50(3H, s); 4.37-4.40(2H, t, J=6.5Hz); 7.71-7.72(2H, d, J=6.4Hz); 8.48-8.50(2H, d, J=6.8Hz).	
[BMPy]PF_6+α-CD[a]	[BMPy]PF_6+β-CD[a]

3.41-3.44 (6H, t, J= 9.00 Hz), 3.45-3.51 (6H, dd, J= 10.00, 3.00 Hz), 3.62-3.67 (18H, m), 3.55-3.61(6H,t, J = 9 Hz), 4.89-4.94 (6H, d, J = 3 Hz); 0.92(3H, s); 1.31-1.38(2H, m); 1.93-2.00(2H, dd, J=8Hz); 2.65(3H, s); 4.47-4.50(2H, t, J=6.5Hz); 7.88-7.90(2H, d, J=6.4Hz); 8.67-8.69(2H, d, J=6.8Hz).	3.41-3.47 (6H, t, J = 9.2 Hz), 3.48-3.53 (6H, dd, J =9.6, 3.2 Hz), 3.53-3.59 (18H, m), 3.62-3.66 (6H, t, J=9.2 Hz), 5.00-5.01 (6H, d, J = 3.6 Hz), 0.95(3H, s); 1.35-1.40(2H, m); 1.96-2.03(2H, dd, J=8Hz); 2.64(3H, s); 4.46-4.50(2H, t, J=6.5Hz); 7.89-7.91(2H, d, J=6.4Hz); 8.83-8.50(2H, d, J=6.8Hz).

[a]Standard uncertainties in temperature: ± 0.01K, Pressure:±10kPa

Table S4. Change in chemical shifts (ppm) of the H3 and H5 protons of cyclodextrin molecule in two different host-guest complexes in D_2O at 298.15 K[a].

Protons of CD	[BMPy]PF_6+α-CD	[BMPy]PF_6+β-CD
H3	0.25	0.20
H5	0.10	0.18

Table S5. Surface Tension (γ) values of α-CD & [BMPy]PF_6, β-CD & [BMPy]PF_6Complexat 298.15 K

CD added (mL)	Total volume (mL)	conc of IL (mM)	conc of CD (mM)	α-CD & [BMPy]PF_6 Complex	β-CD & [BMPy]PF_6 Complex
0	10	10.000	0.00	39.20	39.2
1	11	9.091	0.91	39.72	39.63
2	12	8.333	1.67	40.12	40.04
3	13	7.692	2.31	40.46	40.36
4	14	7.143	2.86	40.78	40.65
5	15	6.667	3.33	41.03	40.92
6	16	6.250	3.75	41.27	41.16
7	17	5.882	4.12	41.50	41.38
8	18	5.556	4.44	41.67	41.56
9	19	5.263	4.74	41.84	41.69

10	20	5.000	5.00	41.98	41.82
11	21	4.762	5.24	42.02	41.88
12	22	4.545	5.45	42.04	41.91
13	23	4.348	5.65	42.06	41.93
14	24	4.167	5.83	42.08	41.95
15	25	4.000	6.00	42.10	41.96
16	26	3.846	6.15	42.12	41.98
17	27	3.704	6.30	42.13	41.99
18	28	3.571	6.43	42.15	42.00
19	29	3.448	6.55	42.17	42.01
20	30	3.333	6.67	42.19	42.02
21	31	3.226	6.774	42.2	42.02
22	32	3.125	6.875	42.21	42.03
23	33	3.031	6.969	42.22	42.03
24	34	2.942	7.058	42.22	42.04

[a]Standard uncertainties in temperature: ± 0.01 K, Pressure: ± 10kPa, surface tension: ±0.02 mNm^{-1}

TableS6. Data for the conductivity study of aqueous $[BMPy]PF_6$+α-CD and $[BMPy]PF_6$+β-CD system (concentration of stock solution of IL = 10mM, concentration of stock solution of CD = 10mM) at 293.15K[a], 303.15K[a], 313.15K[a]

		293.15 K		303.15 K		313.15 K	
conc of IL (mM)	conc of β-CD (mM)	α-CD & $[BMPy]PF_6$ Complex	β-CD & $[BMPy]PF_6$ Complex	α-CD & $[BMPy]PF_6$ Complex	β-CD & $[BMPy]PF_6$ Complex	α-CD & $[BMPy]PF_6$ Complex	β-CD & $[BMPy]PF_6$ ComplexO9
10.000	0.000	0.583	0.583	0.628	0.628	0.680	0.680
9.091	0.909	0.536	0.535	0.576	0.575	0.626	0.613
8.333	1.667	0.491	0.490	0.532	0.530	0.583	0.566
7.692	2.307	0.455	0.454	0.494	0.494	0.547	0.523
7.143	2.857	0.422	0.422	0.458	0.462	0.515	0.491
6.667	3.333	0.397	0.396	0.434	0.436	0.488	0.464
6.250	3.750	0.375	0.374	0.409	0.414	0.465	0.433
5.882	4.117	0.351	0.353	0.387	0.393	0.445	0.411
5.556	4.444	0.331	0.332	0.365	0.372	0.424	0.389
5.263	4.736	0.315	0.314	0.351	0.354	0.407	0.376
5.000	5.000	0.297	0.294	0.337	0.337	0.394	0.358
4.762	5.238	0.294	0.289	0.325	0.326	0.381	0.342

4.545	5.454	0.287	0.284	0.321	0.323	0.378	0.338
4.348	5.652	0.284	0.281	0.320	0.321	0.375	0.335
4.167	5.833	0.280	0.277	0.318	0.316	0.372	0.332
4.000	6.000	0.276	0.273	0.316	0.312	0.368	0.328
3.846	6.153	0.273	0.270	0.314	0.309	0.364	0.324
3.704	6.296	0.270	0.267	0.312	0.306	0.362	0.322
3.571	6.428	0.267	0.264	0.311	0.304	0.360	0.320
3.448	6.551	0.264	0.261	0.309	0.301	0.357	0.317
3.333	6.666	0.262	0.259	0.307	0.300	0.354	0.314
3.226	6.774	0.260	0.257	0.305	0.298	0.354	0.313
3.125	6.875	0.258	0.255	0.304	0.295	0.352	0.312
3.031	6.969	0.256	0.253	0.302	0.292	0.349	0.309
2.942	7.058	0.254	0.251	0.302	0.290	0.347	0.307
2.857	7.143	0.252	0.249	0.299	0.288	0.346	0.306
2.778	7.222	0.252	0.249	0.298	0.286	0.345	0.305
2.703	7.297	0.250	0.247	0.297	0.285	0.343	0.303
2.632	7.368	0.249	0.246	0.296	0.285	0.342	0.302
2.564	7.436	0.248	0.245	0.296	0.285	0.342	0.302

[a]Standard uncertainties in temperature: ± 0.01Kconductivity:± 0.02mS m$^{-1.}$ Pressure:± 10kPa

TableS7. Values of conductivity (κ) at the break point with corresponding concentrations of [BMPy]PF_6 and CDs at 298.15 K[a]

Temperature (K)	Concentration of α-CD (mM)	κ[a]/mS.cm^{-1}	Concentration of β-CD (mM)	κ[a]/mS.cm^{-1}
	[BMPy]PF_6			
293.15	5.106	0.294	5.144	0.290
303.15	5.135	0.327	5.157	0.329
313.15	5.167	0.383	5.192	0.343

[a]Standard uncertainties in temperature:± 0.01K, conductivity: ±0.001 mS·m^{-1}

TableS8. Data for the Benesi-Hildebrand double reciprocal plot performed by UV-VIS spectroscopic study for [BMPy]PF_6-α-CD and [BMPy]PF_6-β-CD systems at 293.15 K

	[Drug] (μM)	[CD] (μM)	A_0	A_1	ΔA	1/ΔA	1/cd
[BMPy]PF_6+ α-CD	50	10	0.4531	0.47203	0.01893	52.8262	100000
	50	20	0.4531	0.48791	0.03481	28.72738	50000
	50	30	0.4531	0.50342	0.05032	19.87281	33333

	50	40	0.4531	0.51473	0.06163	16.22586	25000
	50	50	0.4531	0.53102	0.07792	12.83368	20000
	50	60	0.4531	0.54473	0.09163	10.91346	16667
	50	70	0.4531	0.55285	0.09975	10.02506	14286
	50	80	0.4531	0.56142	0.10832	9.231905	12500
	50	90	0.4531	0.56988	0.11678	8.56311	11111
	50	100	0.4531	0.57948	0.12638	7.912644	10000
	50	10	0.4531	0.47952	0.02642	37.85011	100000
	50	20	0.4531	0.50317	0.05007	19.97204	50000
	50	30	0.4531	0.52531	0.07221	13.8485	33333
	50	40	0.4531	0.54402	0.09092	10.99868	25000
$[BMPy]PF_6$+	50	50	0.4531	0.56834	0.11524	8.677543	20000
β-CD	50	60	0.4531	0.58441	0.13131	7.615566	16667
	50	70	0.4531	0.59856	0.14546	6.874742	14286
	50	80	0.4531	0.60846	0.15536	6.436663	12500
	50	90	0.4531	0.61826	0.16516	6.054735	11111
	50	100	0.4531	0.628606	0.175506	5.697811	10000

Table S9. Data for the Benesi-Hildebrand double reciprocal plot performed by UV-VIS spectroscopic study for $[BMPy]PF_6$-α-CD and $[BMPy]PF_6$-β-CD systems at 298.15 K

	[Drug] (μM)	[CD] (μM)	A_0	A_1	ΔA	$1/\Delta A$	$1/cd$
	50	10	0.44739	0.46263	0.01524	65.6168	100000
	50	20	0.44739	0.47711	0.02972	33.64738	50000
	50	30	0.44739	0.49042	0.04303	23.2396	33333
	50	40	0.44739	0.50273	0.05534	18.07011	25000
$[BMPy]PF_6$+α-CD	50	50	0.44739	0.51502	0.06763	14.78634	20000
	50	60	0.44739	0.52473	0.07734	12.92992	16667
	50	70	0.44739	0.53285	0.08546	11.70138	14286
	50	80	0.44739	0.54142	0.09403	10.6349	12500
	50	90	0.44739	0.54988	0.10249	9.757049	11111

	50	100	0.44739	0.55948	0.11209	8.921402	10000
[BMPy]PF_6+ β-CD	50	10	0.44739	0.47051	0.02312	43.2526	100000
	50	20	0.44739	0.492619	0.045229	22.10971	50000
	50	30	0.44739	0.51342	0.06603	15.14463	33333
	50	40	0.44739	0.53173	0.08434	11.85677	25000
	50	50	0.44739	0.55402	0.10663	9.378224	20000
	50	60	0.44739	0.569273	0.121883	8.20459	16667
	50	70	0.44739	0.58485	0.13746	7.274844	14286
	50	80	0.44739	0.596142	0.148752	6.722599	12500
	50	90	0.44739	0.61588	0.16849	5.93507	11111
	50	100	0.44739	0.62448	0.17709	5.646846	10000

TableS10: Data for the Benesi-Hildebrand double reciprocal plot performed by UV-VIS spectroscopic study for [BMPy]PF_6-α-CD and [BMPy]PF_6-β-CD systems at 303.15 K

	[Drug] (µM)	[CD] (µM)	A_0	A_1	ΔA	$1/\Delta A$	$1/cd$
[BMPy]PF_6+ α-CD	50	10	0.43182	0.4481	0.01628	61.42506	100000
	50	20	0.43182	0.46401	0.03219	31.06555	50000
	50	30	0.43182	0.47842	0.0466	21.45923	33333
	50	40	0.43182	0.49173	0.05991	16.6917	25000
	50	50	0.43182	0.50802	0.0762	13.12336	20000
	50	60	0.43182	0.51873	0.08691	11.50616	16667
	50	70	0.43182	0.52985	0.09803	10.20096	14286
	50	80	0.43182	0.53742	0.1056	9.469697	12500
	50	90	0.43182	0.54988	0.11806	8.470269	11111
	50	100	0.43182	0.559848	0.128028	7.810791	10000
[BMPy]PF_6+	50	10	0.43182	0.454847	0.023027	43.42728	100000

β-CD	50	20	0.43182	0.476417	0.044597	22.42303	50000
	50	30	0.43182	0.49342	0.0616	16.23377	33333
	50	40	0.43182	0.51573	0.08391	11.91753	25000
	50	50	0.43182	0.54002	0.1082	9.242144	20000
	50	60	0.43182	0.558273	0.126453	7.908077	16667
	50	70	0.43182	0.58025	0.14843	6.737183	14286
	50	80	0.43182	0.601142	0.169322	5.905907	12500
	50	90	0.43182	0.62488	0.19306	5.179737	11111
	50	100	0.43182	0.61548	0.18366	5.444844	10000

[a]Standard uncertainties in temperature: ± 0.01 K, Pressure: ± 10kPa.

TableS11. Data obtained from FT-IR spectroscopic study of α-CD, β-CD, $[BMPy]PF_6$,α-CD +$[BMPy]PF_6$, β-CD+$[BMPy]PF_6$.

Group	Wave number (Cm^{-1})				
	α-CD	β-CD	$[BMPy]PF_6$	α-CD+ $[BMPy]PF_6$	β-CD+ $[BMPy]PF_6$
stretching of O-H	3410	3408		3383	3386
stretching of –C-H from $–CH_2$	2935	2941		2932	2931
bending of –C-H from $–CH_2$ and bending of O-H	1421	1404		1385	1388
bending of C-O-C vibration	1165	1160		1152	1154
involving α-1,4linkage	956	954		952	948
Aromatic -C-H Stretching			3142	.....	.....
Stretching –alkyl C-H			3068	.....	.....

stretching of –C-H from $–CH_2$	2965	.....	.....
Stretching -C=N and Stretching -C=C	1647	1638	1636
$-CH_2-$ bending (m)	1469	.....	.....
$-CH_3-$ bending (m)	1385	1371	13781
C-N stretching	1176	1142	1154
out of plane C-H bending	841	830	832

[a]Standard uncertainties in temperature: ± 0.01 K, Pressure: ± 10kPa

TableS12. The observed peaks at different m/z with corresponding ions for the solid inclusion complexes.

Ions	m/z	ions	m/z
$[BMPy]PF_6 + H^+$	296.03	$[BMPy]PF_6 + H^+$	296.03
$[BMPy]PF_6 + Na^+$	318.07	$[BMPy]PF_6 + Na^+$	318.07
$[BMPy]PF_6 + \alpha\text{-CD} + H^+$	1268.92	$[BMPy]PF_6 + \beta\text{-CD} + H^+$	1431.11
$[BMPy]PF_6 + \alpha\text{-CD} + Na^+$	1290.94	$[BMPy]PF_6 + \beta\text{-CD} + Na^+$	1452.87

[a]Standard uncertainties in temperature: ± 0.01 K, Pressure: ± 10kPa

Figures

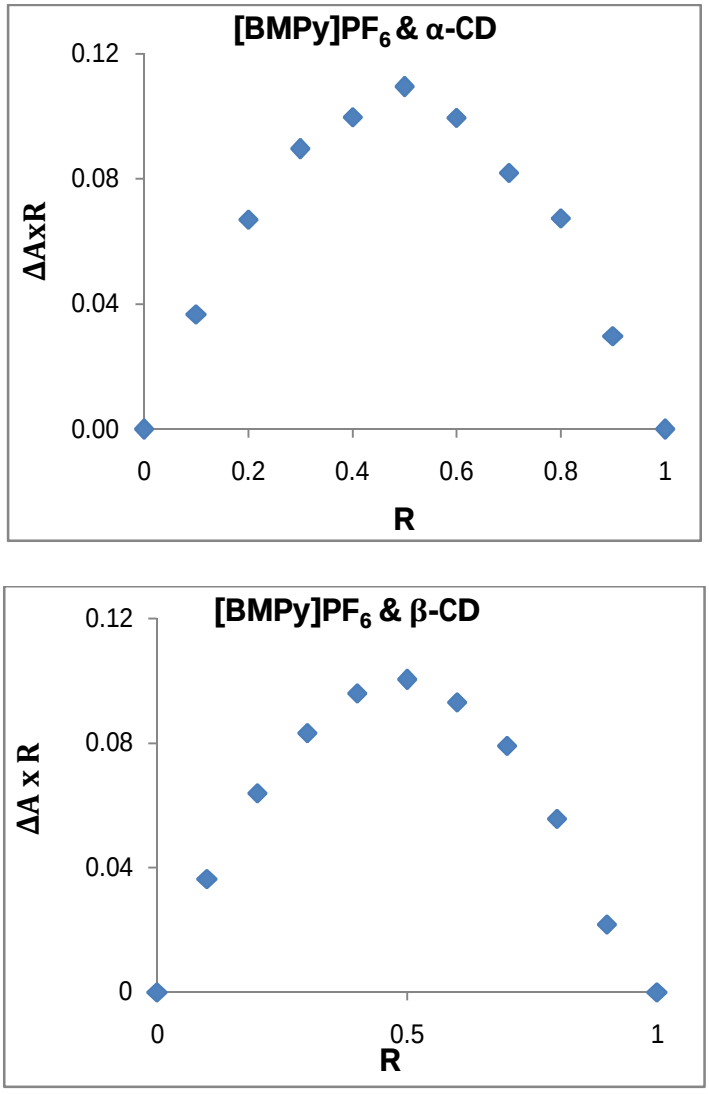

Figure1.Job's Plot for (a) [BMPy]$PF_6$with α-CD and(b)[BMPy]PF_6 with β-CD.

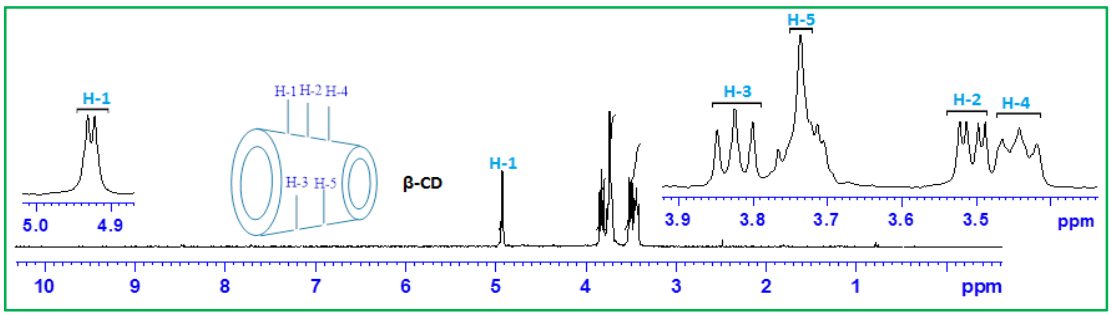

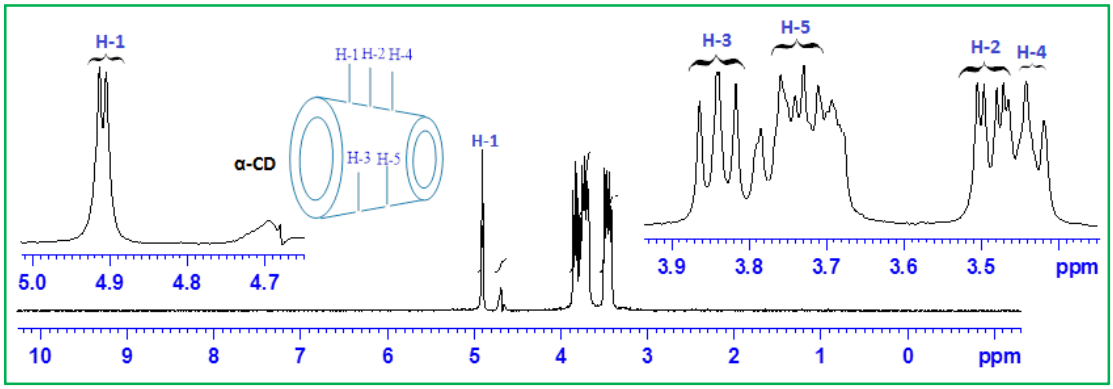
H-1
α-CD
H-1 H-2 H-4
H-3 H-5
H-1
H-3
H-5
H-2
H-4
5.0 4.9 4.8 4.7
3.9 3.8 3.7 3.6 3.5 ppm
10 9 8 7 6 5 4 3 2 1 0 ppm

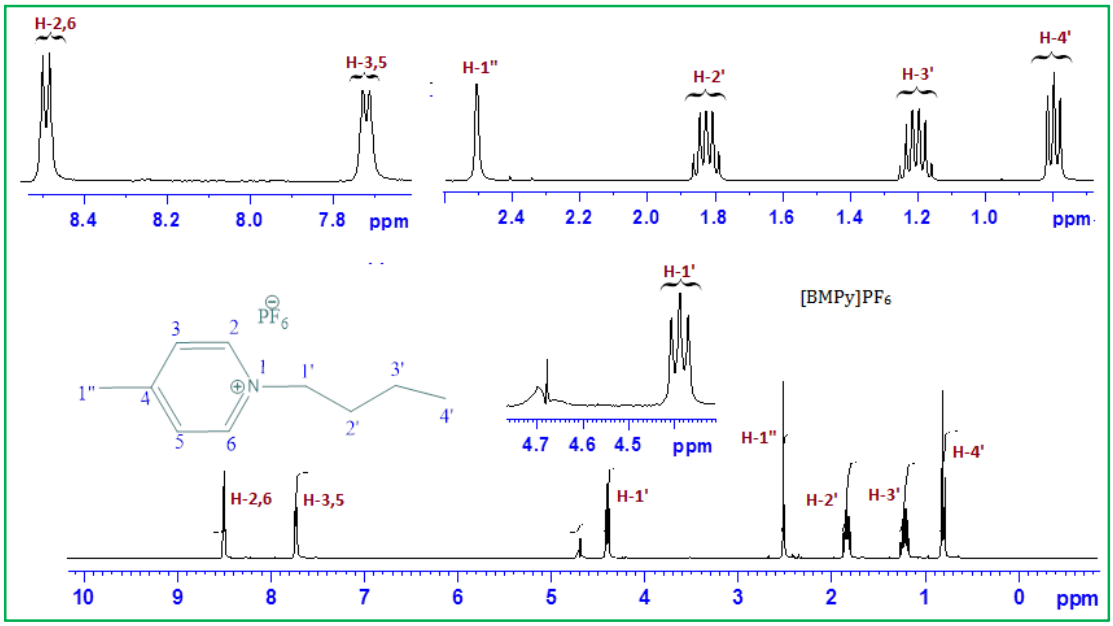
H-2,6
H-3,5
H-1"
H-2'
H-3'
H-4'
8.4 8.2 8.0 7.8 ppm
2.4 2.2 2.0 1.8 1.6 1.4 1.2 1.0 ppm
[BMPy]PF6
H-1'
4.7 4.6 4.5 ppm
10 9 8 7 6 5 4 3 2 1 0 ppm

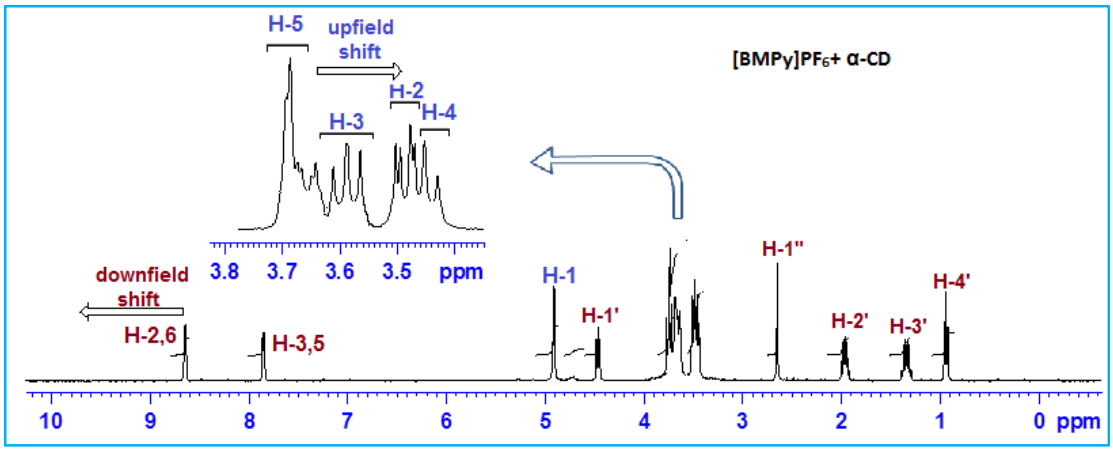
H-5
upfield shift
H-2
H-3
H-4
[BMPy]PF6+ α-CD
3.8 3.7 3.6 3.5 ppm
downfield shift
H-2,6
H-3,5
H-1
H-1'
H-1"
H-2'
H-3'
H-4'
10 9 8 7 6 5 4 3 2 1 0 ppm

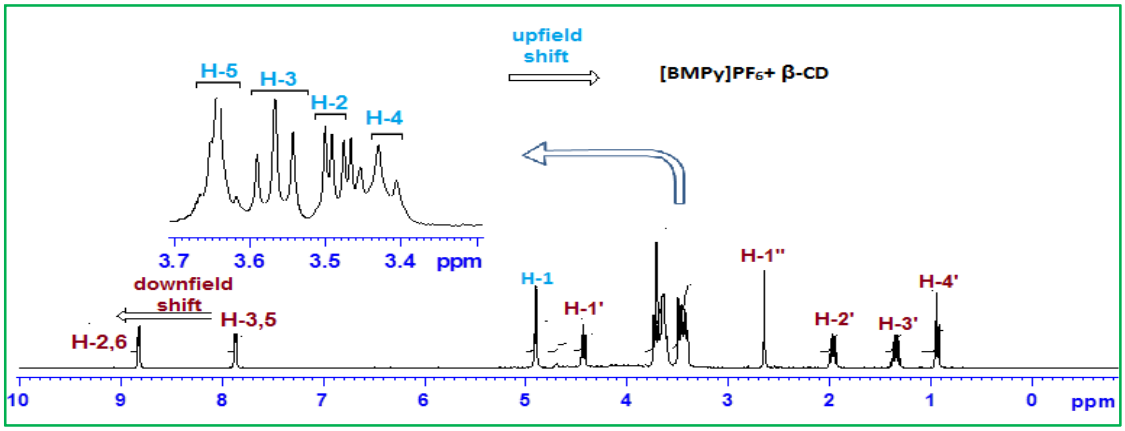

Figure2.^{1}H NMR spectra of pure α-CD, β–CD, [BMPy]$PF_6$and [BMPy]PF_6+α-CD and [BMPy]PF_6+β–CD. (In D_2O, 400 MHz)

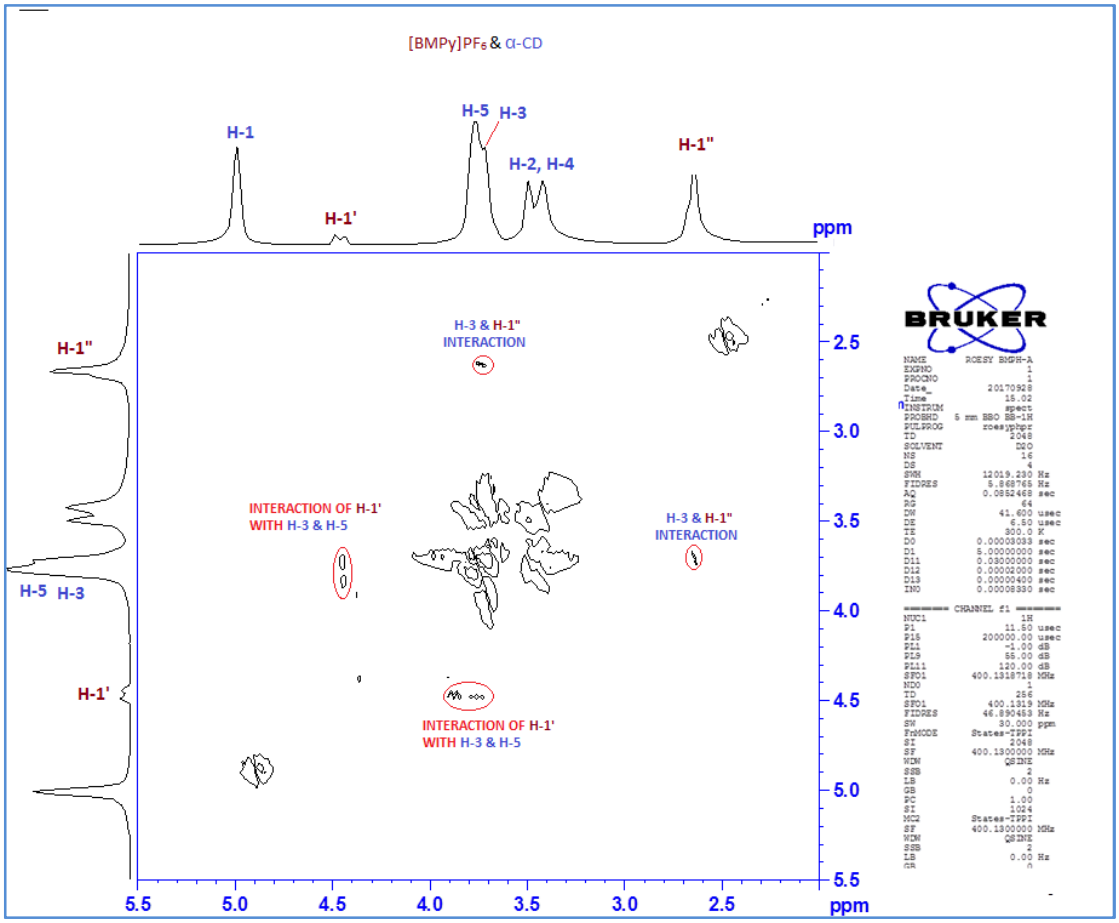

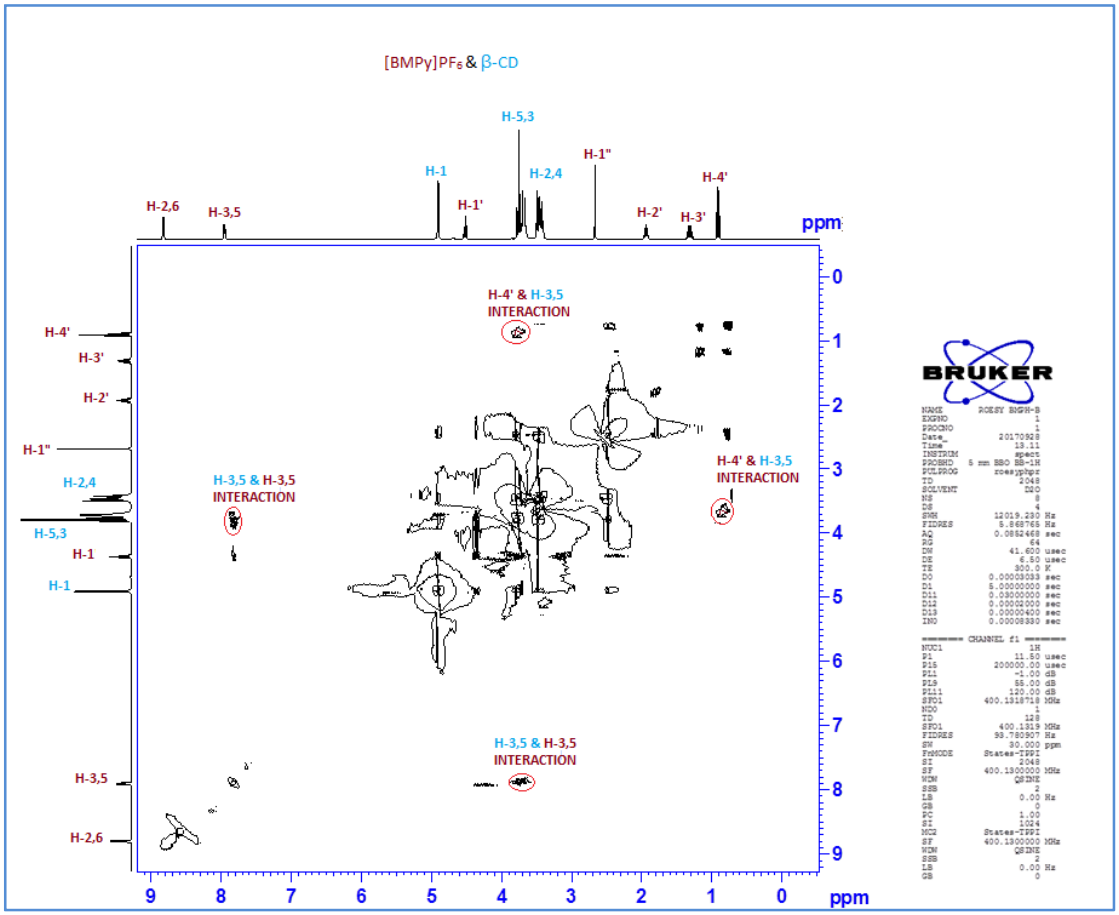

Figure3.2D ROESY spectra of the solid ICs of [BMPy]PF_6-α-CD AND[BMPy]PF_6-β-CD in D2O. (Cross correlations are indicated by red circles)

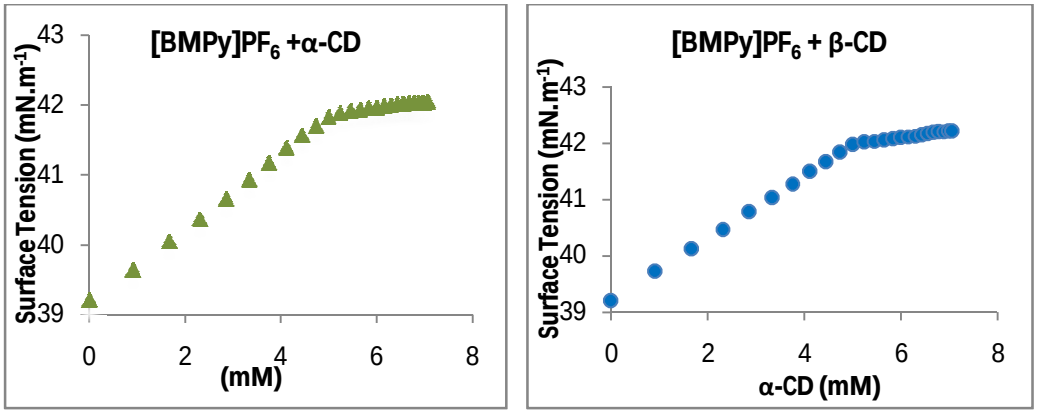

Figure4. Surface tension of [BMPy]$PF_6$with α –CD, [BMPy]PF_6 with β–CD at 298.15 K.

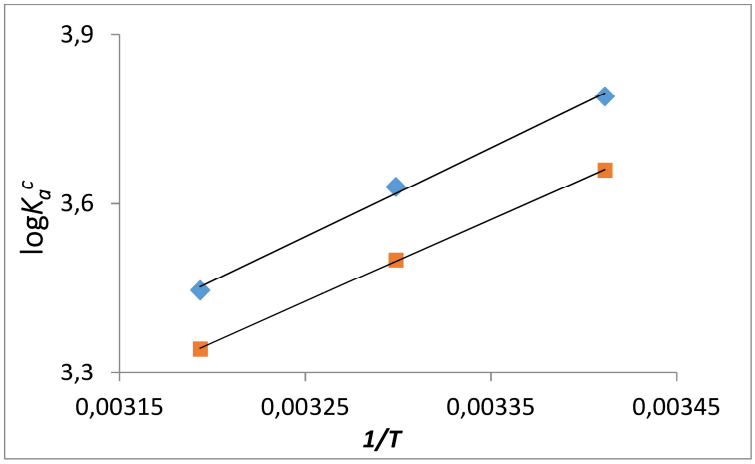

Figure5(a). Plot of $\log Ka^c$ vs 1/T for the interaction of α-CD with $[BMPy]PF_6$ (♦) and β-CD with $[BMPy]PF_6$(■).

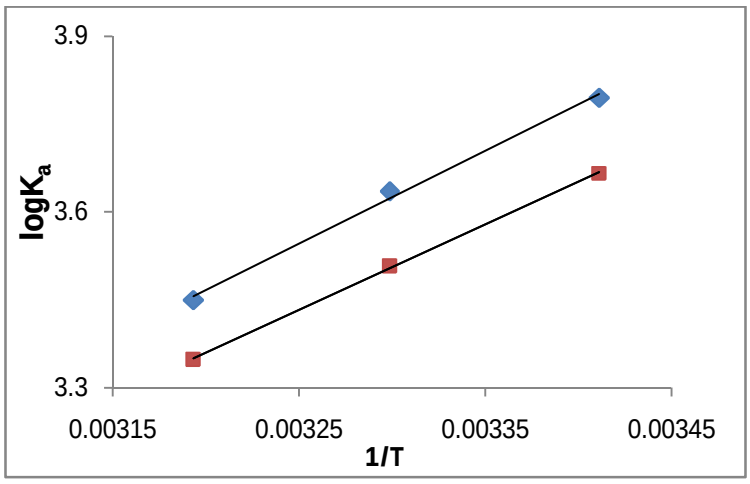

Figure5(b). Plot of $\log Ka^c$ vs 1/T for the interaction of α-CD with $[BMPy]PF_6$ (♦) and β-CD with $[BMPy]PF_6$(■).

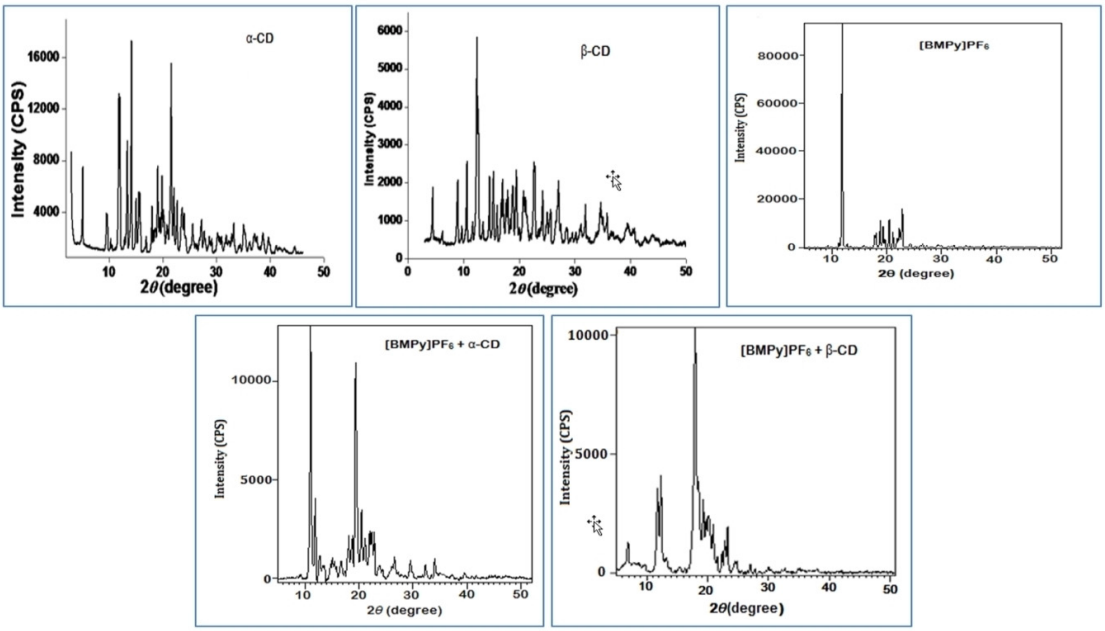

Figure6. Powder X-Ray diffraction pattern of [BMPy]PF6, α-CD, β-CD, [BMPy]PF6+α-CD and [BMPy]PF6 +β-CD (1:1 stoichiometry) inclusion complex

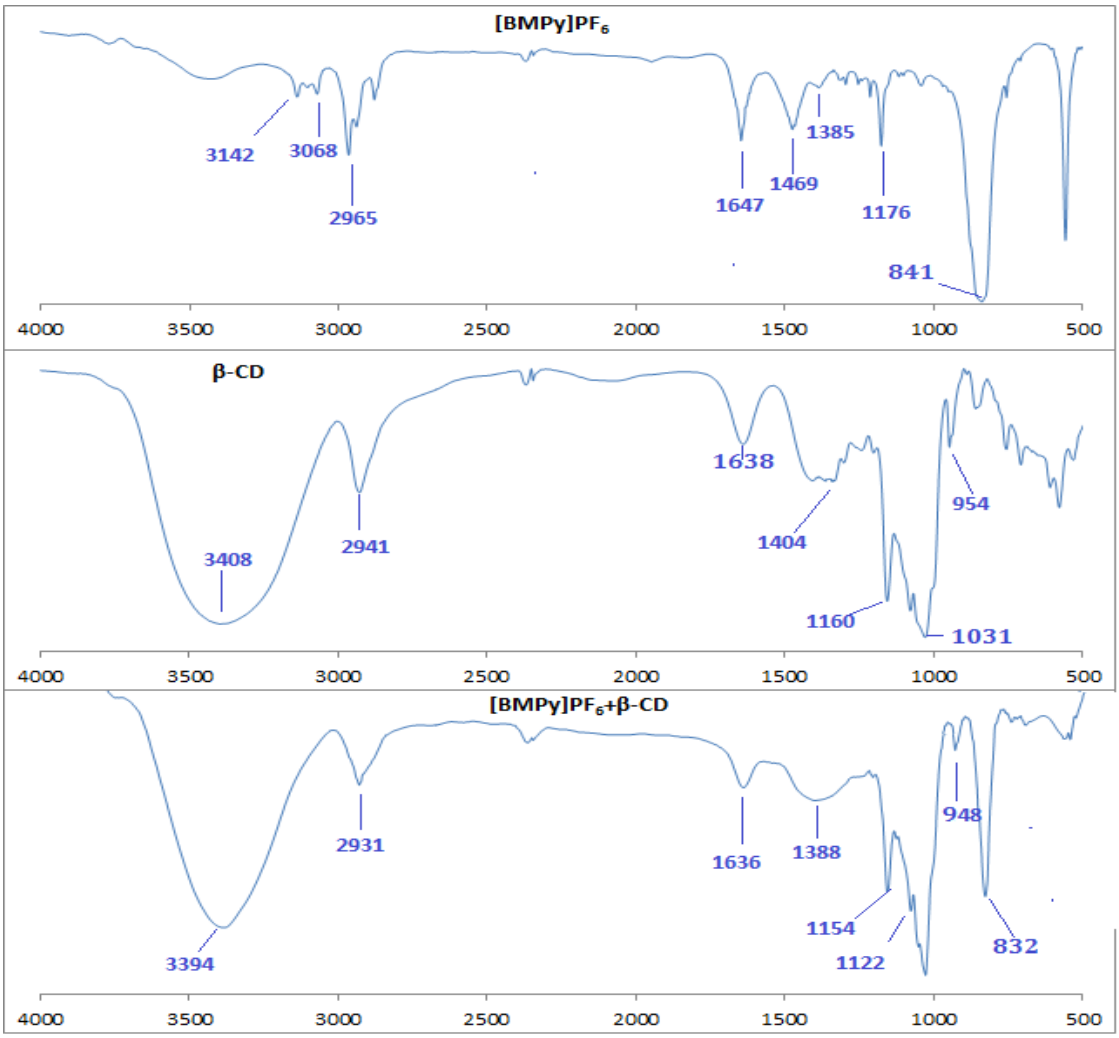

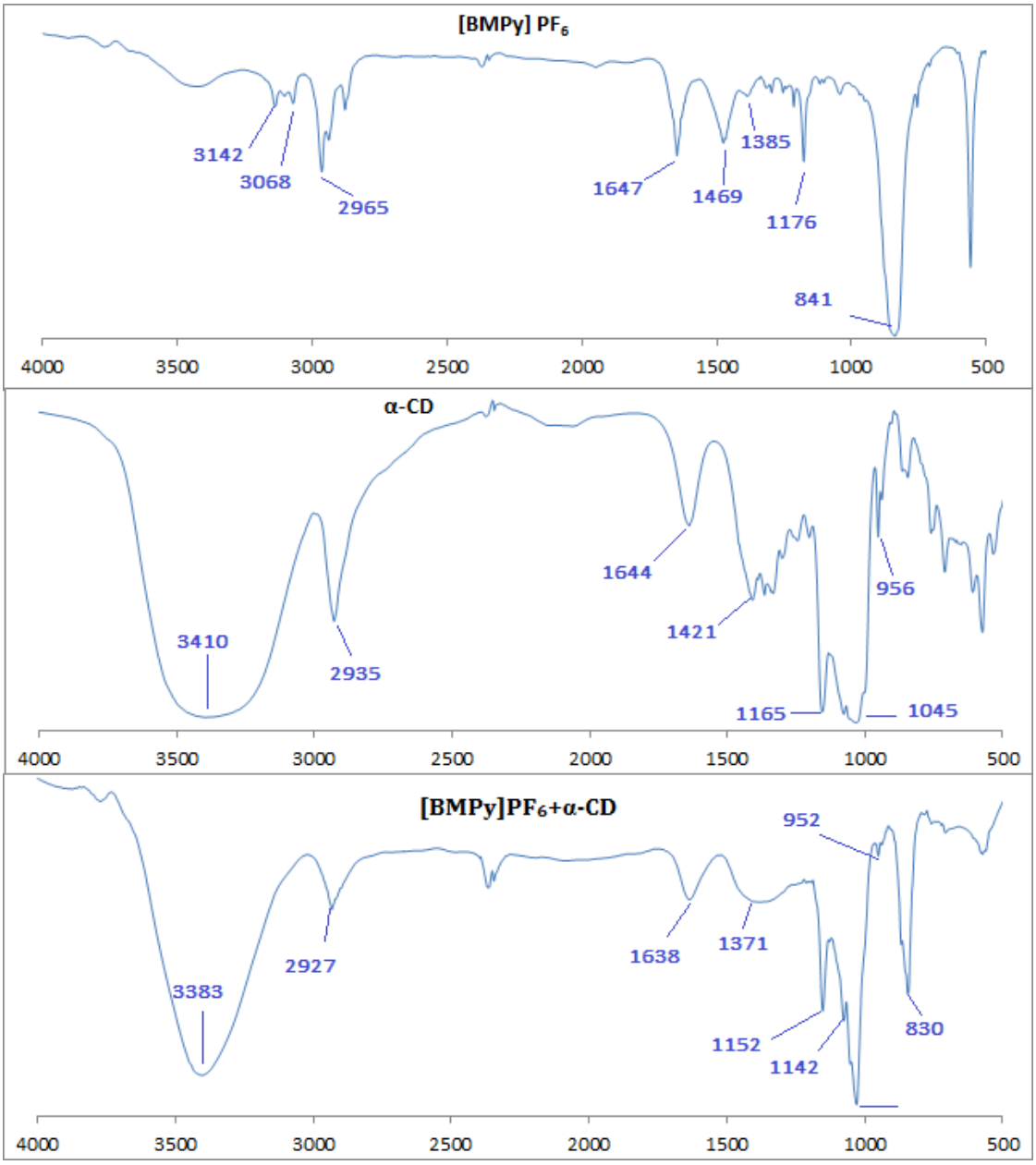

Figure7. FT-IR spectra of freeα-CD, β-CD, [BMPy]PF_6 and their 1:1incluusion complexes ([BMPy]PF_6+α-CD) and ([BMPy]PF_6+β-CD) at 298.15K.

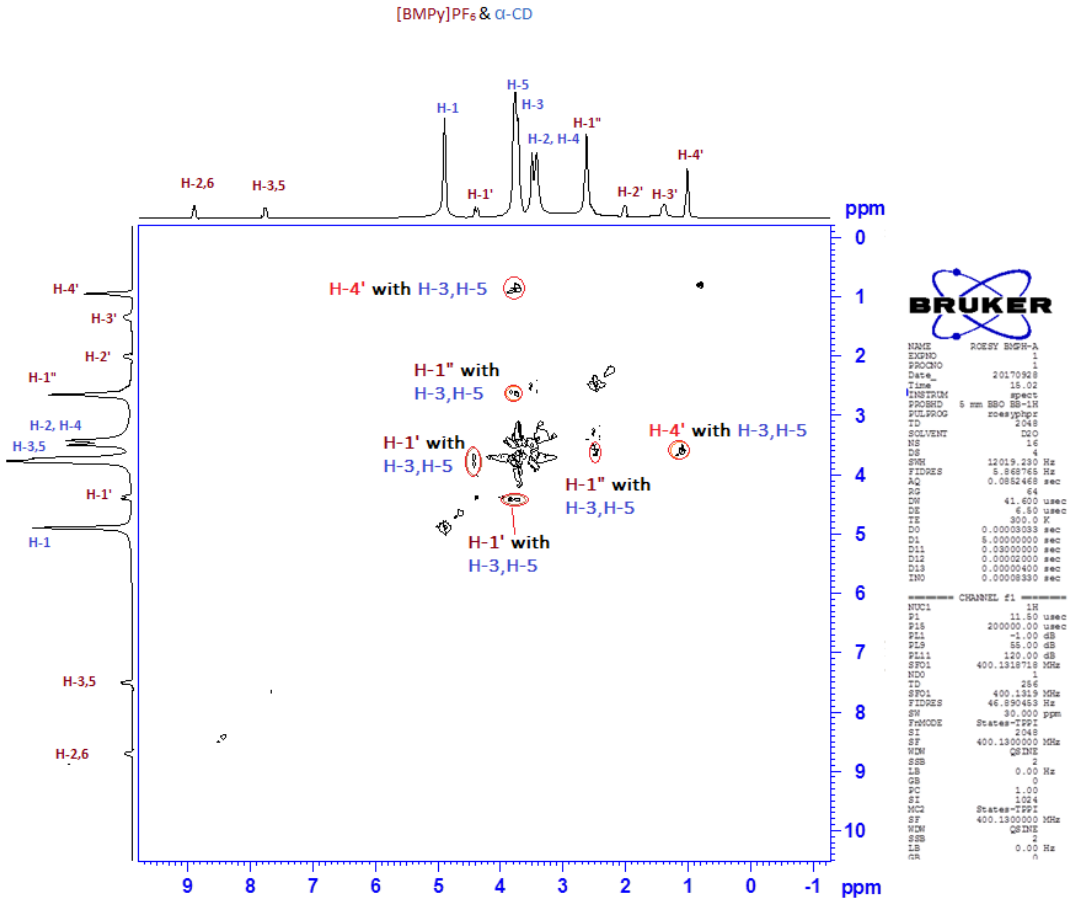

FigureS1. 2D ROESY spectra of the solid ICs of [BMPy]PF_6-α-CD in D_2O. (Cross correlations are indicated byred circles)

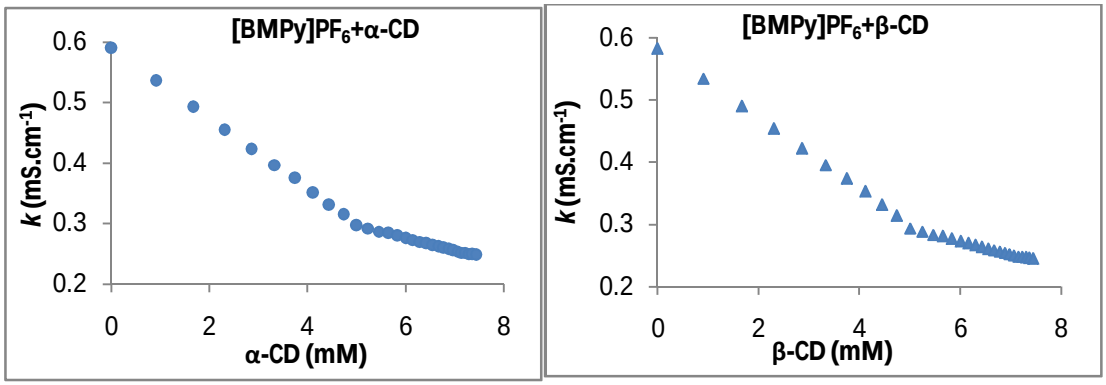

(a)

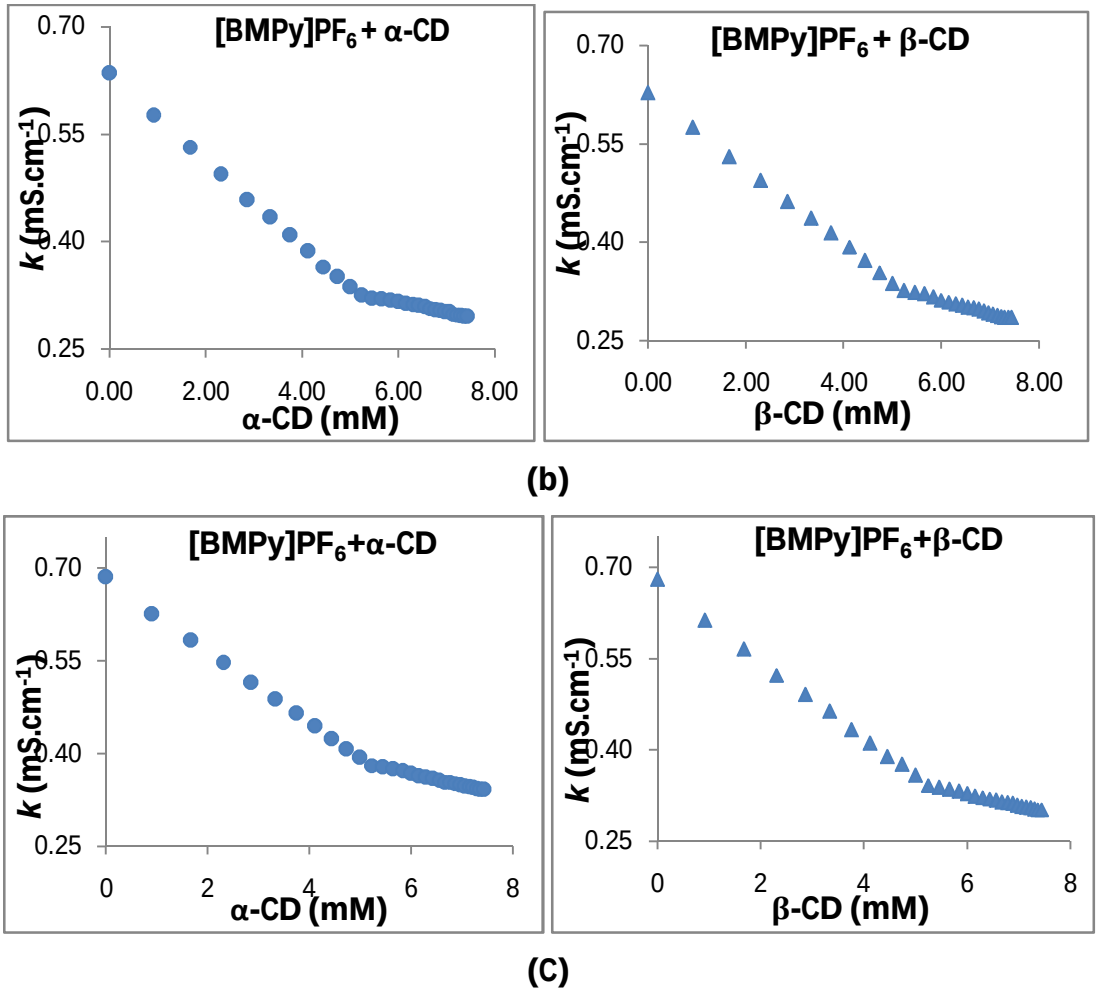

FigureS2. Plot of conductivity with increasing concentration of α-CD andβ-CD with [BMPy]PF_6+α-CD and [BMPy]PF_6+β-CD at (a) 293.15 K, (b) 303.15K and (c) 313.15K.

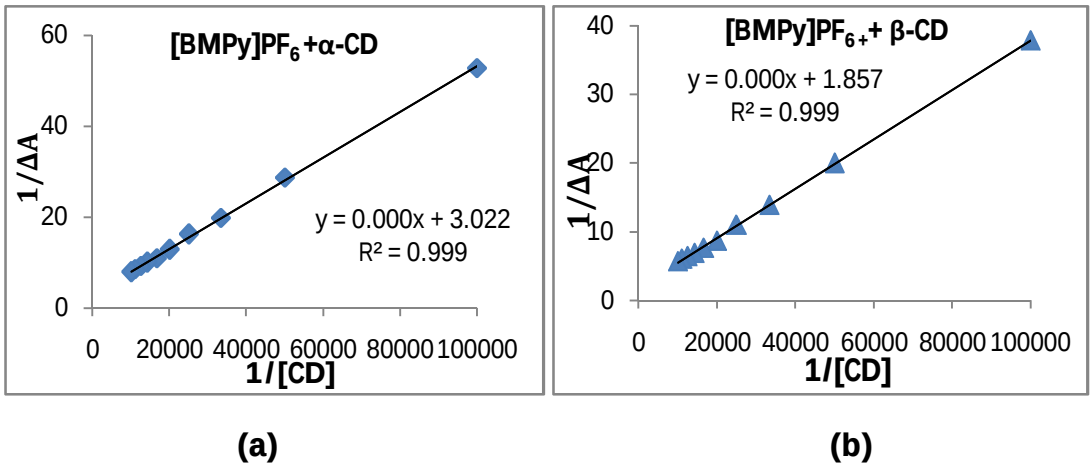

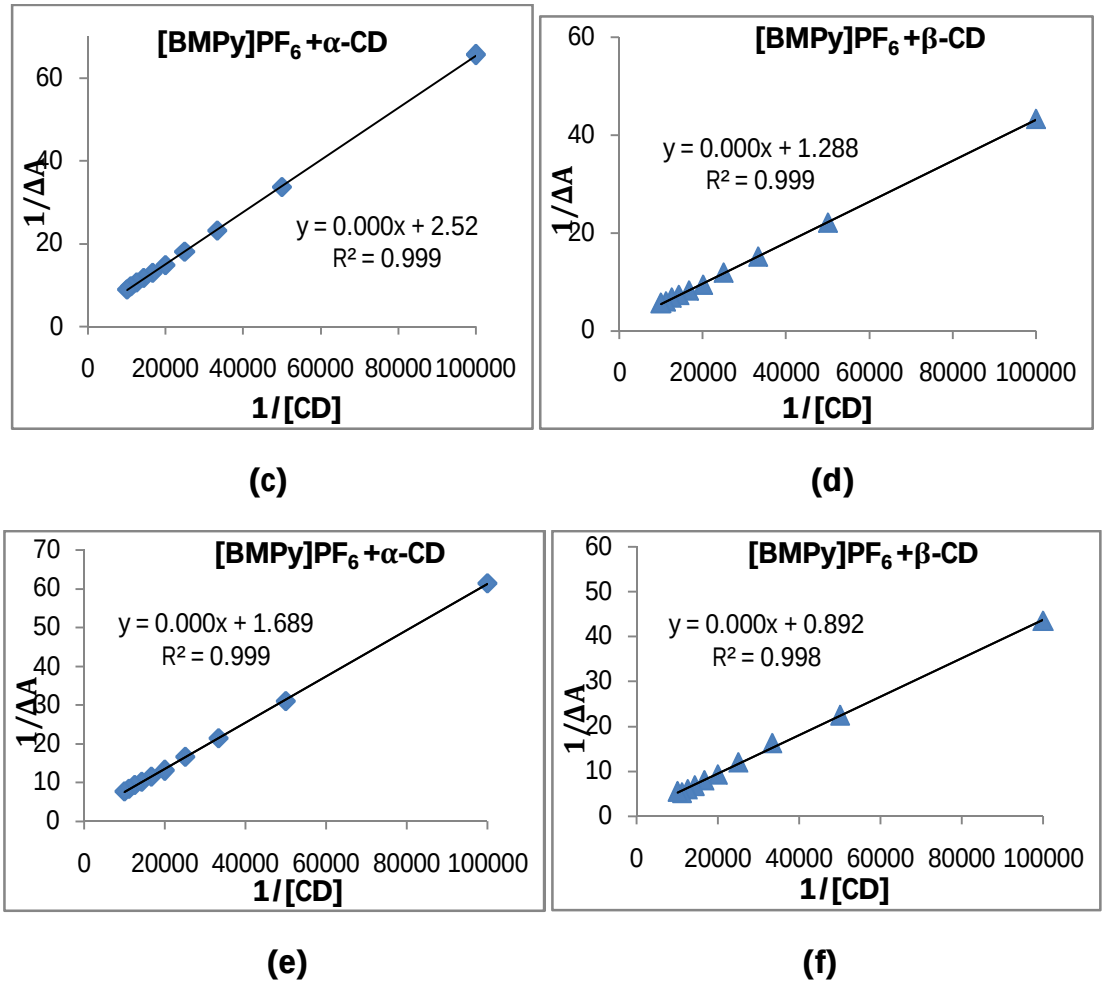

FigureS3. Benesi-Hildebrand double reciprocal plots for the effect of *β*-CD on the absorbance of [BMPy]PF_6 +β-CD and [BMPy]PF_6+α-CD (252 nm) at different temperatures(a) and (b) shows at 293015K, (c) and (d) at 303.15K and (e) and (f) at 313.15K.

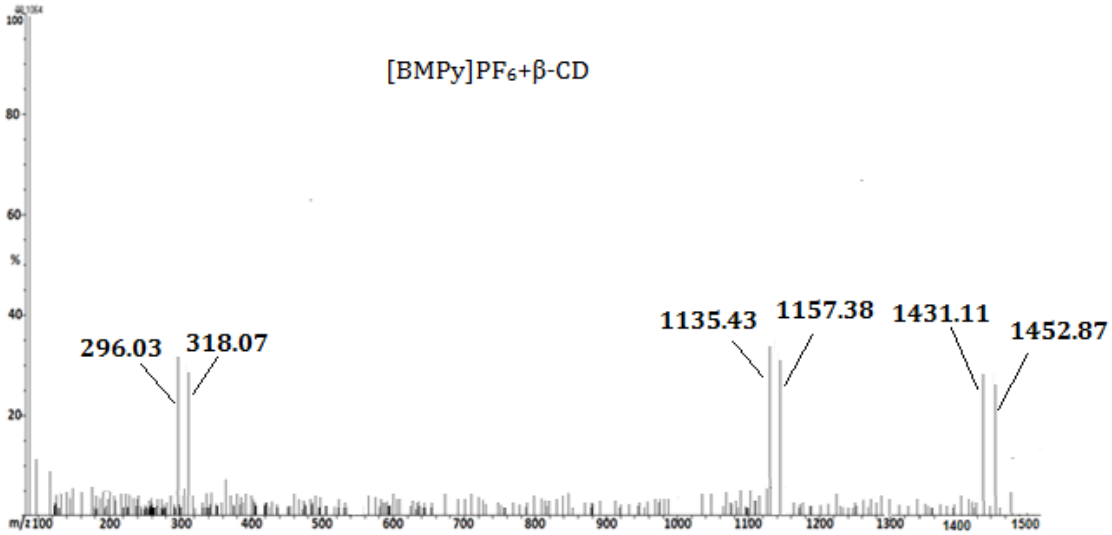

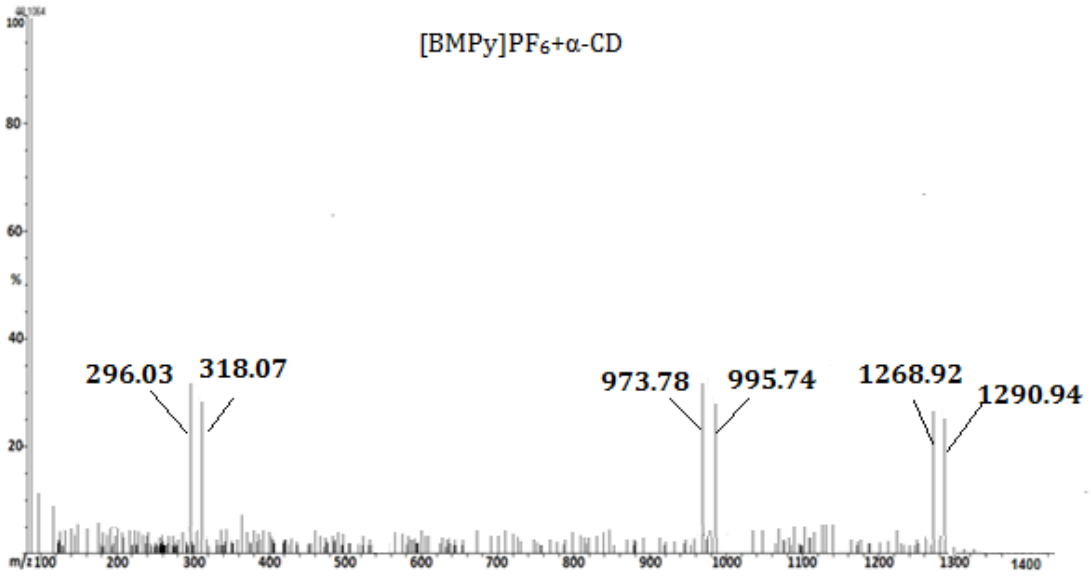

FigureS4. ESI mass spectra of [BMPy]PF_6-β-CD and [BMPy]PF_6-α-CD inclusion complex.

Scheme

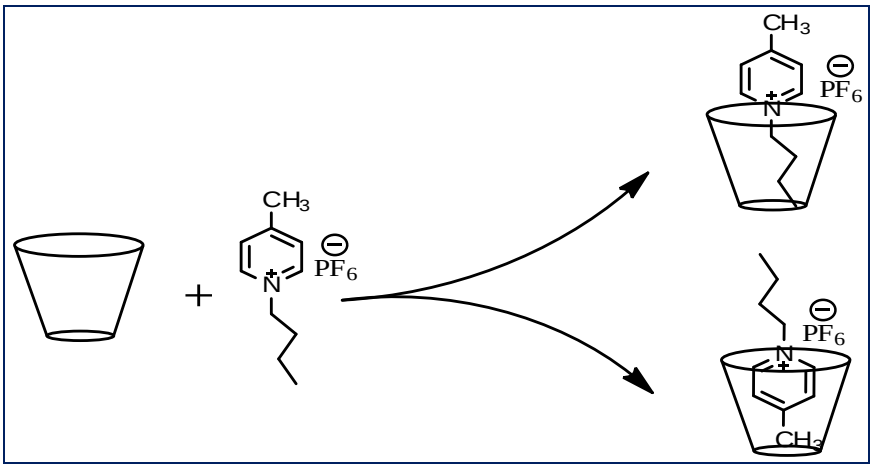

Scheme1. Schematic representation of the inclusion of [BMPy]PF_6 with Cyclodextrin in mixed solvent media.